Marine Pollution Bulletin 154 (2020) 111125

Contents lists available at ScienceDirect

Marine Pollution Bulletin

journal homepage: www.elsevier.com/locate/marpolbul

Contamination and ecological risk assessment of the Red Sea coastal sediments, southwest Saudi Arabia

Ali Kahal[a], Abdelbaset S. El-Sorogy[a,b,*], Saleh Qaysi[a], Sattam Almadani[a], Osama M. Kassem[c], Ahmed Al-Dossari[a]

[a] Geology and Geophysics Department, College of Science, King Saud University, Saudi Arabia
[b] Geology Department, Faculty of Science, Zagazig University, Egypt
[c] National Research Center, Geology Department, Dokki, Cairo, Egypt

ARTICLE INFO

Keywords:
Contamination
Ecological risk assessment
Heavy metals
Jazan
Red Sea coast
Saudi Arabia

ABSTRACT

The level of heavy metals (HMs) in coastal sediments has attracted the environmental researchers due to their persistence, abundance, biomagnification and toxicity. The present study was conducted to assess the contamination and ecological risk assessment of HMs in Jazan coastal sediments, Red Sea, Saudi Arabia utilizing pollution indices and multivariate statistical analyses. A total of 32 surface samples were collected for Cu, Sb, Zn, Cr, Cd, Pb, Fe, Co, Ni, Al, and total organic matter analysis using an atomic absorption spectrophotometer. The results indicate the following descending order of metal concentrations: Al > Fe > Cr > Cu > Zn > Ni > Co > Pb > Cd > Sb. Average level of Cd is significantly higher than those from many neighboring and worldwide coastal sediments; and recorded very severe enrichment, severe contamination and very high risk in the investigated sediments. The pollution indices and statistical analyses revealed that proportion of Zn, Fe, Ni, Cr, Al, Cu, Sb and Pb were formed from lithogenic sources of weathering Quaternary units and atmospheric deposition. Most of the Cd, Sb, and Pb levels were derived from anthropogenic sources of industrial, agricultural, and fishing activities. The higher contribution of organic matter may be attributed to the mangrove roots and organic fertilizers; and played a key role in adsorbing, transferring and accumulating of elements.

1. Introduction

Human activities have a significant negative impacts on the coastal regions and marine food resources. The conservation of aquatic organisms and marine environment from pollution are imperative issue for monitoring the aquatic environments (Pejman et al., 2015). In a consequence of their non-biodegradation, biomagnification and toxicity, HMs are considered as a serious contamination in marine sediments, and are related to the industrial emissions, commercial fertilizers, fuel combustion using sewage sludges, urban and agricultural activities and dumping, and treatment of wastes (He et al., 2005).

As a result of the growth of urbanization, industrialization, and agriculture during the past decades and their excessive release of various HMs into the Red Sea coastal water, many studies have been done on their coastal sediments and marine skeletons of both sides of the Egyptian and Saudi Arabia (e.g. Beltagy, 1984; Abd El-Wahab and El-Sorogy, 2003; El-Sorogy et al., 2012, 2013a, 2013b, 2016; Usman et al., 2013; Salem et al., 2014; Youssef and El-Sorogy, 2016; Nour et al., 2018, 2019; Kahal et al., 2018).

Heavy metal contamination has been observed in some coastal regions of the Red Sea on the Saudi Arabian site, especially in the northwest area (e.g. Al-Farawati et al., 2011; Youssef and El-Sorogy, 2016; Kahal et al., 2018). However, the studies are still scarce in the southwest coastal area. Many of the HMs are extremely toxic and could move up through the marine food chain, from seagrass, algae and marine organisms into fish, and humans. Therefore, the objectives of the present study are: (1) to assess the HMs contamination in Jazan coastal sediments, Saudi Arabia using some credible pollution indices, (2) to specify the major sources of investigated metals (anthropogenic or natural sources) by multivariate statistical techniques, (3) to document the present status of HMs contamination in sediments to control and protect the biota and aquatic environment.

* Corresponding author at: Geology and Geophysics Department, College of Science, King Saud University, Saudi Arabia.
E-mail address: asmohamed@ksu.edu.sa (A.S. El-Sorogy).

https://doi.org/10.1016/j.marpolbul.2020.111125
Received 11 December 2019; Received in revised form 27 February 2020; Accepted 28 March 2020
Available online 09 April 2020
0025-326X/

2. Material and methods

2.1. Study area

The study area lies along the Red Sea coast, southwest of the Saudi Arabia, between 42° 76′ 36″ - 42° 24′ 06″ E and 16° 48′ 84″ - 17° 49′ 91″ N (Fig. 1). The coastline is differentiated into sandy-dominated, mangrove-dominated and rocky dominated beaches (Supplementary data, Table 1). The sandy-dominated beaches are represented in the investigated area by 14 samples (43.75%) and are composed of fine to coarse sand of detrital origin, which derived from the hinterland. Sometimes include coral, bivalve, gastropod, foraminifer, crustacean, bryozoan and sea grass fragments. The mangrove-dominated beaches are represented by 12 samples (37.50%). These beaches may be formed in bays sheltered from waves and tidal currents or in high wave activity and currents. The sediments are composed of fine to medium sand, silty clay, clayey silt and clay fractions, and rare shell fragments. The rocky-dominated beaches are rare and represented by 6 samples (18.75%) and are composed of man-made concrete seawalls and rocky blocks to protect residential areas from wave action. Surveying through collecting samples along the studied Jazan coastline indicated human activities, representing by crowded fishing boats, landfilling, sewage effluents and different solid wastes.

2.2. Analytical methods

Thirty-two samples were collected from the coastal and subtidal zone (from 0 to 30 cm deep) of the Jazan coastal area (Fig. 1), using a grab sampler. Most of the sampled sediments consist of silt and sand, but there are some individuals of clay or containing a high proportion of clay (Table 1). Methods from the US Environmental Protection Agency (EPA/CE- 81-1 Protocol) were followed for the sample

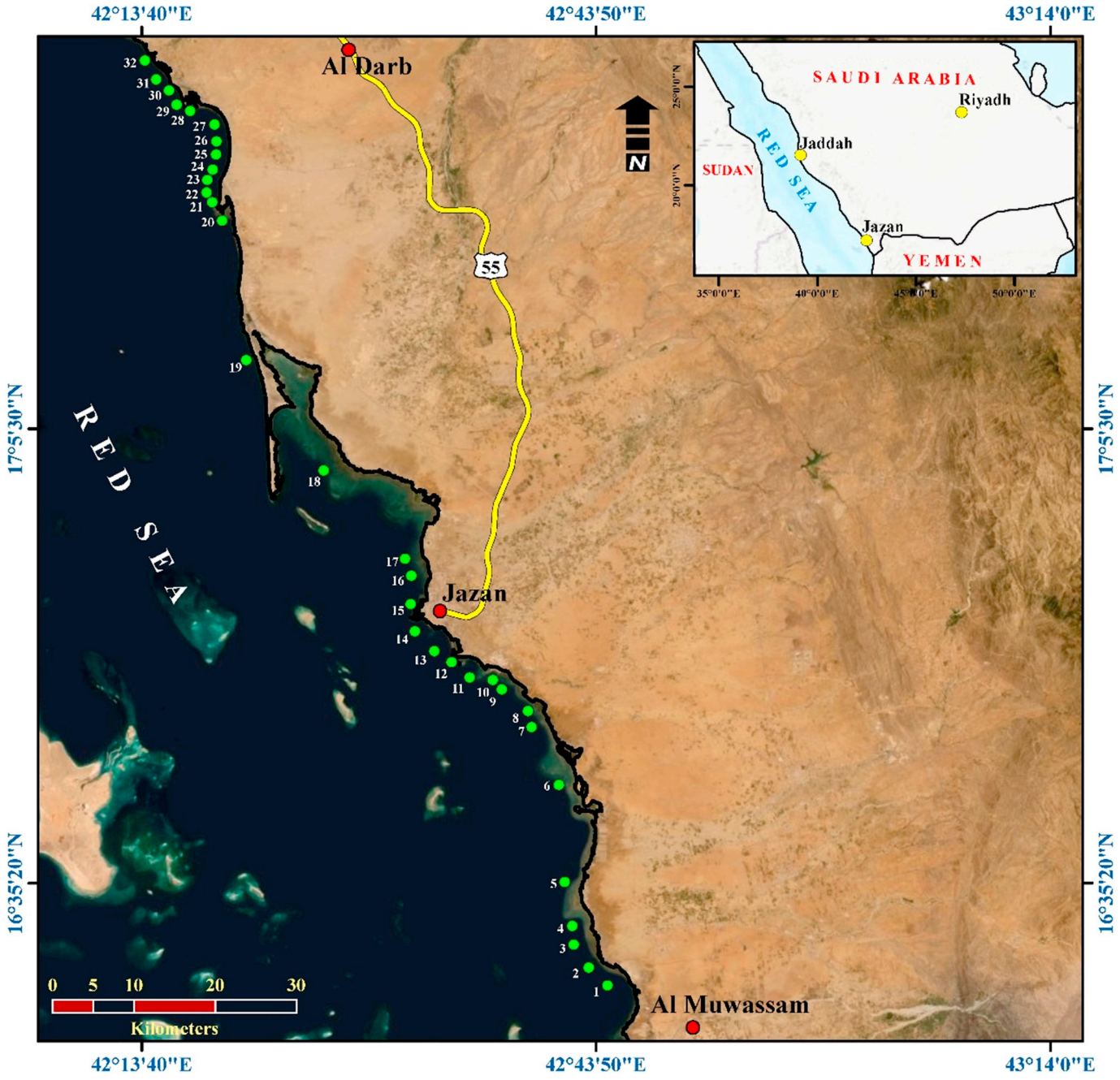

Fig. 1. Location map of the study area and samples location.

Table 1
Location, sediment type and concentrations of 10 metals (μg/g) and organic matter (%) in the 32 surface sediments along the Jazan coastline.

S.N.	Latitudes	Longitudes	Sediment type	Al	Cr	Fe	Co	Ni	Cu	Zn	Cd	Sb	Pb	O.M.
1[a]	16 48 84	42 76 36	Clayey silt	2022	32.1	1962	3	22.4	32.2	28.2	0.48	0.2	1.6	2.22
2[a]	16 50 08	42 74 03	Fine sandy clay	8105	34.2	4462	3.5	23.3	43.2	38.9	0.79	0.52	4.2	1.98
3[b]	16 53 35	42 72 63	Clayey silt	2682	23.8	1388	2.6	13.5	21.2	18.5	0.52	0.24	2.2	2.25
4[b]	16 55 40	42 72 48	Fine sandy clay	1998	33.6	1992	2.8	22.9	32.8	30	0.46	0.22	1.6	2.02
5[a]	16 60 26	42 71 63	Fine sand	2052	32.3	1966	3.3	24.1	32.6	29.2	0.44	0.18	1.5	1.66
6[b]	16 70 45	42 70 90	Fine sandy clay	2695	24.1	1390	2.5	13.3	22.1	18.7	0.54	0.21	2.1	3.18
7[b]	16 76 79	42 67 81	Fine sandy clay	2038	33.5	2002	3.2	24.5	32.8	28.8	0.42	0.2	1.8	1.98
8[b]	16 78 56	42 67 40	Black silty clay	2700	25.2	1402	2.2	14.2	21.9	20	0.56	0.18	1.9	3.12
9[b]	16 80 93	42 64 51	Fine sandy clay	2678	25	1382	2.4	12.8	21.5	19.4	0.58	0.21	2.1	2.98
10[b]	16 81 98	42 63 51	Fine to medium sand	7902	34.5	4455	3.7	23.6	44	38.2	0.76	0.5	4.4	1.94
11[b]	16 82 26	42 60 96	Fine to medium sand	2036	33.8	2002	2.8	23.8	33.6	29.1	0.42	0.23	2	1.88
12[a]	16 83 96	42 58 97	Fine sand	6412	40.8	4422	10.1	22	28.8	31.2	0.24	0.14	1.9	2.05
13[c]	16 83 49	42 57 43	Fine to medium sand	2002	34.6	1007	2.2	17.3	36.6	28.9	0.52	0.31	2.1	2.18
14[c]	16 87 36	42 54 89	Fine sandy clay	2045	33.3	1971	3.1	23.5	32.4	28.5	0.44	0.2	1.8	1.82
15[c]	16 90 38	42 54 42	Fine sandy clay	7105	32.5	4332	3.8	23.8	44	40.2	0.82	0.52	4.2	1.98
16[c]	16 93 52	42 54 50	Clayey silt	2705	23.8	1399	2.8	14	23.2	19.3	0.51	0.18	2.2	3.14
17[c]	16 95 40	42 53 80	Fine to medium sand	2122	32.6	2018	3.6	25.2	33.4	28.2	0.48	0.26	2.4	1.96
18[c]	17 01 17	42 53 31	Black clay	2688	24	1386	2.3	13.8	21	20.2	0.63	0.22	2.4	3.12
19[b]	17 02 75	42 52 68	Fine sandy clay	1995	35	1998	3.2	24	33.1	31.5	0.48	0.2	1.7	1.88
20[b]	17 04 12	42 47 90	Clayey silt	8008	35.2	4398	3.8	24.5	44.2	40.1	0.92	0.55	4.6	2.04
21[b]	17 07 56	42 44 10	Black silty clay	2680	23.5	1408	2.7	13.6	21.8	18.2	0.58	0.26	2	3.02
22[a]	17 14 74	42 42 07	Fine sandy clay	7222	35.2	3352	5.2	16.3	25.2	22.4	0.43	0.22	2.1	2.22
23[a]	17 36 70	42 31 50	Fine sandy clay	6405	40	4495	8.8	22.8	30	32.4	0.22	0.14	1.8	2.08
24[a]	17 37 84	42 32 10	Fine sandy clay	1988	33.6	1015	2.4	16.8	37	30.2	0.54	0.36	2.4	2.24
25[a]	17 39 51	42 32 47	Fine to coarse calc. sand	2014	34	998	2.2	18.1	36.4	28.6	0.55	0.3	2.1	2.45
26[a]	17 40 96	42 32 53	Fine to medium calc. sand	6398	39.8	4498	9.6	22.8	28.2	32.6	0.24	0.18	1.5	1.98
27[a]	17 42 84	42 32 31	Fine to coarse sand	2008	35.4	1012	2.5	18	38.2	30	0.52	0.35	1.9	2.18
28[a]	17 44 33	42 29 62	Fine to medium sand	6422	41.4	4518	9.8	23.1	29.4	31.7	0.22	0.16	1.7	1.92
29[b]	17 45 02	42 76 36	Clayey sand	2134	34.1	2021	3.6	26	33.8	29.2	0.5	0.32	2.4	2.04
30[a]	17 46 06	42 27 26	Fine to medium sand	6400	40.8	4522	10.2	24.2	20.4	32	0.25	0.18	1.9	2.06
31[a]	17 47 81	42 25 85	Fine to coarse sand	1998	36	1010	2.2	17.3	36.6	27.6	0.56	0.33	2.1	2.24
32[a]	17 49 91	42 24 06	Fine to coarse sand	2014	34.2	997	2	16.8	38	28.9	0.52	0.28	2	2.26
Minimum				1988	23.5	997	2	12.8	20.4	18.2	0.22	0.14	1.5	1.66
Maximum				8105	41.4	4522	10.2	26	44.2	40.2	0.92	0.55	4.6	3.18
Average				3817	32.9	2432	4.13	20.0	31.6	28.5	0.51	0.27	2.3	2.26

O.M., organic matter (%).
[a] Sandy-dominated beaches.
[b] Mangrove-dominated beaches.
[c] Rocky-dominated beaches.

preparation and handling. Cu, Zn, Cd, Al, Pb, Fe, Co, Sb, Cr, and Ni analyses were conducted using an atomic absorption spectrophotometer (GBC 932, Ver1.1) in laboratories of King Saud University, College of Science. The samples were air dried at 60 °C and passed through a 63 sieve for achieving fine-grained sediment. 0.2 g of each sample were digested in Teflon cups for about 2 h in mixture of 1 HF, 2 $HClO_4$ and 3 HNO_3 acids and left overnight to complete digestion. Moreover, a sequential weight loss at 550 °C (Dean, 1974) was used to determine the total organic matter (%TOM). The enrichment factor (EF), contamination factor (CF), potential contamination index (Cp), geoaccumulation index (Igeo), soil pollution index (SPI), and potential ecological risk index (PERI) were used as pollution indices to detect the sources of metals (Table 2). Moreover, statistical analyses were performed by using SPSS 16.0 statistical software and Microsoft Excel 2016.

3. Results and discussion

3.1. Levels of HMs and worldwide comparison

Table 1 summarizes the concentration of 10 HMs and total organic matter in 32 surface sediments from the Jazan coastal area. Al is the most abundant HMs (average of 3816.65 μg/g), followed by Fe (2432.32 μg/g), Cr (32.85 μg/g), Cu (31.59 μg/g), Zn (28.51 μg/g), Ni (20.03 μg/g), Co (4.13 μg/g), Pb (2.31 μg/g), Cd (0.51 μg/g), and Sb (0.27 μg/g). The average organic matter content (2.26%) is much higher than 0.95% and 1.76%, which recorded from the northwest Red Sea coast and the Dammam Al-Jubail area, Saudi Arabia respectively (Kahal et al., 2018; El-Sorogy et al., 2018). This indicates the contribution from mangrove roots and decayed leaves, algae, and organic fertilizers on the land. The spatial distribution of HMs within the investigated area indicates high levels in some individual samples without a fixed trend (Fig. 2). Sb, Cu, Zn, Cd, and Pb exhibited the same distribution pattern, particularly in recording high levels in samples 2, 10, 15, and 20 (Fig. 2A, B). Co and Cr recorded high values in samples 12, 23, 26, 28, and 30 (Fig. 2B, C), while Fe and Al in samples 2, 10, 12, 15, 20, 23, 28, and 30 (Fig. 2D). Ni exhibited a fluctuating pattern, with high levels in samples 2, 5, 7, 11, 15, 17, 20, 29 and lower ones in samples 3, 6, 9, 16, 18, and 21 (Fig. 2E).

Table 3 illustrates a comparison between our metal average levels and other levels in worldwide coastal areas, as well as the sediment quality guidelines (SQGs). The values of SQGs consist of a threshold effect concentration (TEC, lower value) and a probable effect concentration (PEC, higher value). Values below TEC were considered as no-low risk; these between TEC and PEC were considered as medium risk; and as high risk when they were higher than PEC (Duodu et al., 2016; Yu et al., 2012; Mao et al., 2019). Cd level was higher than the other levels mentioned in Table 4, except those of Nour and El-Sorogy

Table 2
Pollution indices used in the present study and their classifications.

Pollution indicators	Procedures of calculation and classifications						
Enrichment factor(EF)	EF = (M/Fe) sample/(M/Fe) background (M/Fe) sample is the ratio of metal and Fe concentrations in the sample, and (M/Fe) background is the ratio of metal and Fe concentrations in the Earth's crust. Birch (2003) determined seven classes of EF in sediments.						
	EF < 1 No enrichment	EF < 3 Minor enrichment	EF = 3–5 Moderate enrichment	EF = 5–10 Moderately severe enrichment	EF = 10–25 Severe enrichment	EF = 25–50 Very severe enrichment	EF > 50 Extremely severe enrichment
Geoaccumulation Index (Igeo)	$Igeo = Log_2 (Cn/(1.5 \times Bn))$ Cn is the measured concentration of metal (n) in the sediments, Bn is the geochemical background concentration of the metal (n) in shale, and 1.5 is introduced to minimise the effects of possible variations in the background values. Müller (1981) determined seven classes of Igeo in sediments:						
	Igeo < 0 Unpolluted	0 < Igeo < 1 Unpolluted to moderately polluted	1 < Igeo < 2 Moderately polluted	2 < Igeo < 3 Moderately to strongly polluted	3 < Igeo > 4 Strongly polluted	4 < Igeo < 5 Strongly to very strongly polluted	Igeo > 5 Very strongly polluted conditions
Contamination Factor (CF)	$C_f = C_o/C_b$ Co is the sediment metal content in the sample and Cb is the normal background value of the metal. Hökanson (1980) classified CF into four groups:						
	Cf < 1 Low contamination factor	1 ≤ Cf < 3 Moderate contamination factor	3 ≤ Cf < 6 Considerable contamination factor	Cf ≥ 6 Very high contamination factor			
Potential contamination index (Cp)	CP = Cmax/Cb Cmax is the maximum concentration of a metal in sediment, and Cb is the average value of the same metal in a background level. Cp values are classified into three categories.						
	Cp < 1 Low contamination	1 < Cp < 3 Moderate contamination	Cp > 3 Severe or very severe contamination				
Potential Ecological Risk Index (PERI)	$\overset{n}{\underset{i}{PERI}} = \sum (Trf \times CF)$ Trf is the toxic response factor for metals are in the order; Zn = Co = 1, Cr = 2, Cu = Pb = 5, Ni = 6, Sb = 10 and Cd = 30. The degree of ecological risk can be classified into five classes (Hökanson, 1980; Qing et al., 2015; Tang et al., 2017).						
	PERI < 40 No~low risk	40 ≤ PERI < 80 Moderate risk	80 ≤ PERI < 160 Considerable risk	160 ≤ PERI < 320 High risk	PERI ≥320 Very high risk		
Soil Pollution Index (SPI)	SPI = Cs/Cm where, Cs is the concentration of metal in the sample and Cm is the permissible levels of metals in sediments (USEPA, 1983). The level of each heavy metal was classified into three classes.						
	SPI ≤ 1 Low contamination	1 < SPI ≤ 3 Moderate contamination	SPI > 3 High contamination				

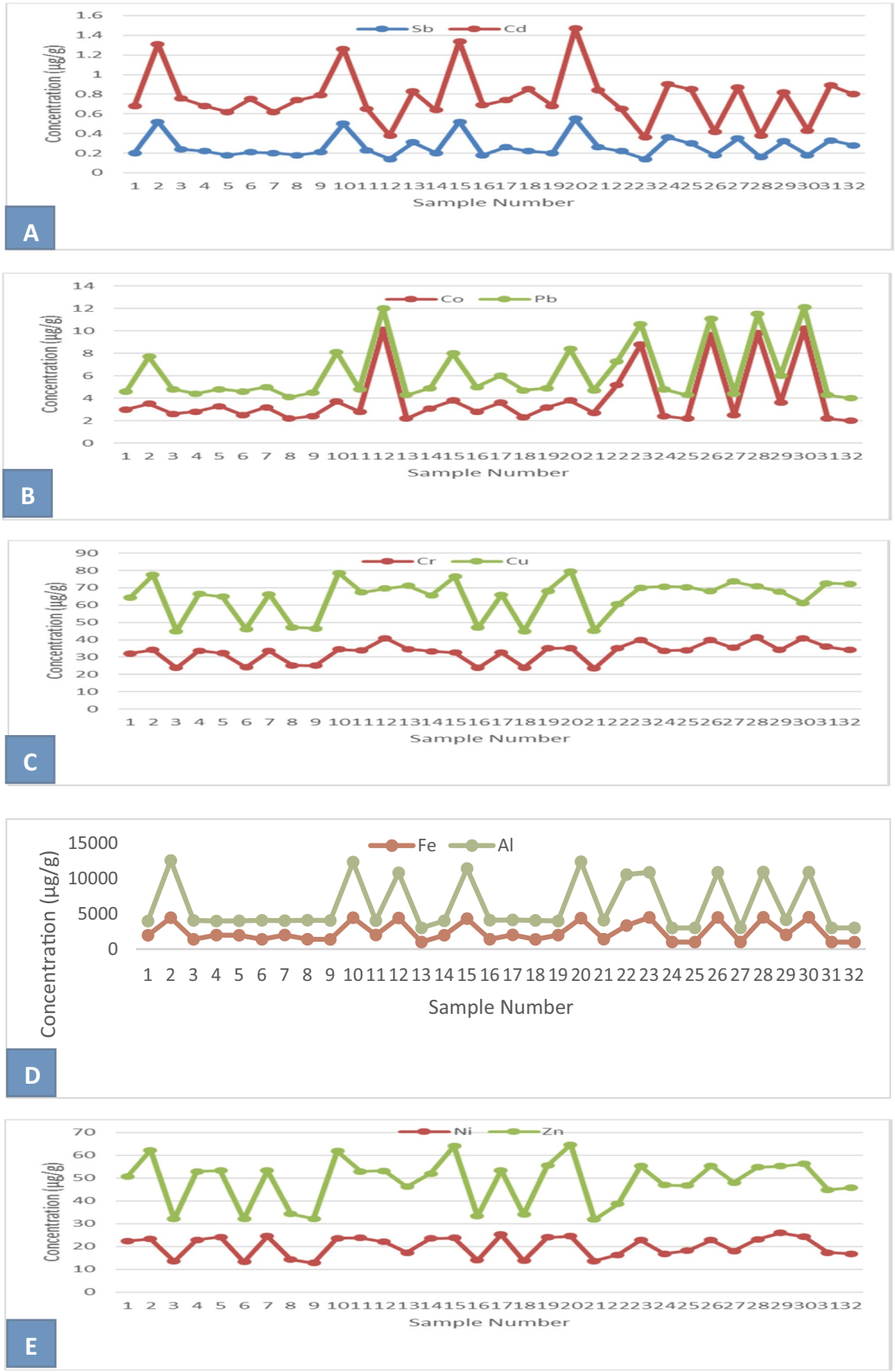

Fig. 2. Spatial distribution of HMs within the studied coastal sediments. A. Sb and Cd; B. Co and Pb; C. Cr and Cu; D. Fe and Al; E. Ni and Zn.

Table 3
Comparison between the metal concentrations (μg/g) in the studied sediments and those in other worldwide sites.

Location		Fe	Ni	Zn	Cu	Co	Al	Cr	Sb	Cd	Pb	Reference
Jazan coastal area, Red Sea, Saudi Arabia		2432.32	20.03	28.51	31.59	4.13	3816.65	32.85	0.27	0.51	2.31	Present study
Shalatein coastal area, Red Sea, Egypt		8451.62	17.52	44.15	9.43	3.927				0.534	11.43	Nour et al. (2019)
Tajan River, Iran		5005.3	8.2	19.7		4.2						Alahabadi and Malvandi (2018)
Al-Khobar, Arabian Gulf, Saudi Arabia		7552	75.10	52.68	182.97	4.75	2020	51.03		0.226	5.358	Alharbi and El-Sorogy (2017)
Red Sea coast, Saudi Arabia			10.06	20.85	5.73	4.01				0.25		Ruiz-Compean et al. (2017)
Red Sea coast, Saudi Arabia		1413.34	13.66	16.75	18.67	5.34	4876.56	20.18		0.18	3.54	Kahal et al. (2018)
Arabian Gulf, Saudi Arabia		8474.21	77.07	48.26	297.29	4.01	1887.07	63.79		2.13	5.25	El-Sorogy et al. (2018)
Gokcekaya Dam Lake, Turkey		15,495	125.7	265.8	108.99	85.57		216.65		0.007	74.44	Akin and Kırmızıgu (2017)
Mediterranean Sea, Libya		2084	22.65	26.36	17.30	5.95				0.83	11.69	Nour and El-Sorogy (2017)
Red Sea coast, Egypt		3490	11.404	22.636	1.938	9.696				0.102	3.255	Salem et al. (2014)
Background shale		47,200	68	95	45	19	80,000	90		0.3	20	Turekian and Wedepohl (1961)
Background continental crust		56,300	75	70	55	25	82,300	100		0.2	12.5	Taylor (1964)
Daliao River System, China		26,100	22.6	71.8	20.0	10.2		43–45		0.34	26.6	Lin et al. (2012)
Sediment quality guidelines	TEC		23	121	32			43.4	2	0.99	35.9	Mao et al. (2019)
	PEC		49	459	149			111	25	4.98	128	

Table 4
Minimum, maximum and average values of the different pollution indices in the present study.

Metals	EF			Igeo			CF			PI			ERI	Cp
	Min.	Max.	Aver.	Min.	Max.	Aver.	Min.	Max.	Aver.	Min.	Max.	Aver.	Sum	
Pb	0.79	5.58	2.84	−2.30	−1.18	−1.93	0.08	0.23	0.12	0.15	0.46	0.23	18.15	0.23
Cd	7.66	87.23	45.39	−0.02	1.41	0.75	0.73	3.07	1.69	0.29	1.21	0.67	1568	3.06
Zn	3.32	14.78	7.54	−1.36	−0.57	−0.94	0.19	0.42	0.30	0.36	0.80	0.57	9.59	0.42
Ni	3.38	12.59	7.26	−1.38	−0.67	−0.96	0.19	0.38	0.29	0.32	0.65	0.50	56.67	0.38
Sb	0.98	11.16	4.72	−2.08	−0.72	−1.50	0.09	0.37	0.18	0.26	1.04	0.51	57	0.37
Cu	4.73	39.98	18.52	−1.73	−0.61	−1.14	0.45	0.98	0.70	0.58	1.26	0.90	112.18	0.98
Co	1.95	6.14	4.33	−3.83	−1.48	−3.01	0.11	0.54	0.22	0.25	1.28	0.52	6.74	0.54
Cr	3.93	18.69	18.69	−1.06	1.05	−0.64	0.26	0.46	0.36	0.24	0.41	0.33	23.38	0.46

(1917) and Nour et al. (2019). Average value of Cu was higher than those from the Egyptian Red Sea coast, Saudi Red Sea coast, Libyan Mediterranean coast, Chinese Daliao River System (Salem et al., 2014; Nour et al., 2019; Ruiz-Compean et al., 2017; Kahal et al., 2018; Nour et al., 2019; Nour and El-Sorogy, 2017; Lin et al., 2012). Cr value was lower than the other values mentioned in Table 4, except that from the northwest Red Sea coast by Kahal et al. (2018).

Zn and Ni values were greater than the values recorded from the Iranian Tajan River and the Saudi Red Sea coast (Alahabadi and Malvandi, 2018; Ruiz-Compean et al., 2017; Kahal et al., 2018). The average values of Co and Pb were much less than those from Turkish Gokcekaya Dam Lake, Background shale and Chinese Daliao River System (Akin and Kırmızıgu, 2017; Turekian and Wedepohl, 1961; Lin et al., 2012). Our levels of Ni, Zn, Cu, Cr, Sb, Cd, and Pb were less than those of the maximum effect concentration (TEC) of the SQGs (Table 3).

3.2. Ecological risk assessment of HMs and possible sources

Table 4 illustrates the minimum, maximum and average values of the pollution indices used in this work. Cadmium (Cd) recorded very severe enrichment, severe contamination and very high risk (average EF = 45.39 and CP = 4.06 and PERI = 1568). Cu indicated severe enrichment and considerable risk (average EF = 18.52 and PERI = 112.18). Cr recorded severe enrichment (average EF = 18.69). There is a significant difference between the results of SQGs, Cp and SPI in one hand, and those of EF and PERI in the other hand. The largest difference lies in Cd, Cr and Cu, where SQGs, Cp and SPI suggest no risk for the studied sediments, the other two methods show medium to extreme risk. This implies that although the total concentrations of Cd, Cr and Cu are relatively low, because they were mostly driven from anthropogenic sources, the high toxicity and mobility of them in sediments can lead to high risk to the Jazan coastal area. In general, the average concentration of some metals, like Fe and Al in the sampling area is lower than the background concentration. Relatively small range of metal distribution indicates that these metals are mainly from natural sources (Mao et al., 2019).

Dendrogram using average linkage subdivided the studied HMs into two different groups (Fig. 3). Each group revealed common sources under certain physiochemical circumstances, and similar behaviors during transformations. The first group contains Cd, Sb, Pb, Co, Cu, Zn, Cr, Ni, and OM, which mainly implying industrial activities around the Jazan coastline. Presence of OM in this group suggests that organic materials play a key role in adsorbing, transferring and accumulating of the mentioned elements (Aghadadashi et al., 2019). The second group includes Fe and Al, of lithogenic origin, where Al and Fe are well-defined markers for natural erosion of crustal materials (Mil-Homens et al., 2014; Mao et al., 2019).

In addition, the dendrogram between sample locations and the analyzed metals subdivided the 32 samples into two similar low linkage distance clusters (Fig. 4). The first cluster contains samples 1, 3, 4, 5, 6, 7, 8, 9, 11, 13, 14, 16, 17, 18, 19, 21, 24, 25, 27, 29, 31 and 32. Except sample 29, which recorded the highest value of Ni (26 μg/g), samples of this cluster include the lowest values of Al, Cr, Fe, Co, Ni, Zn, Cd, Sb, and Pb (Table 1). The second cluster includes the samples 2, 10, 12, 15, 20, 22, 23, 26, 28 and 30. The most samples of this cluster contain the

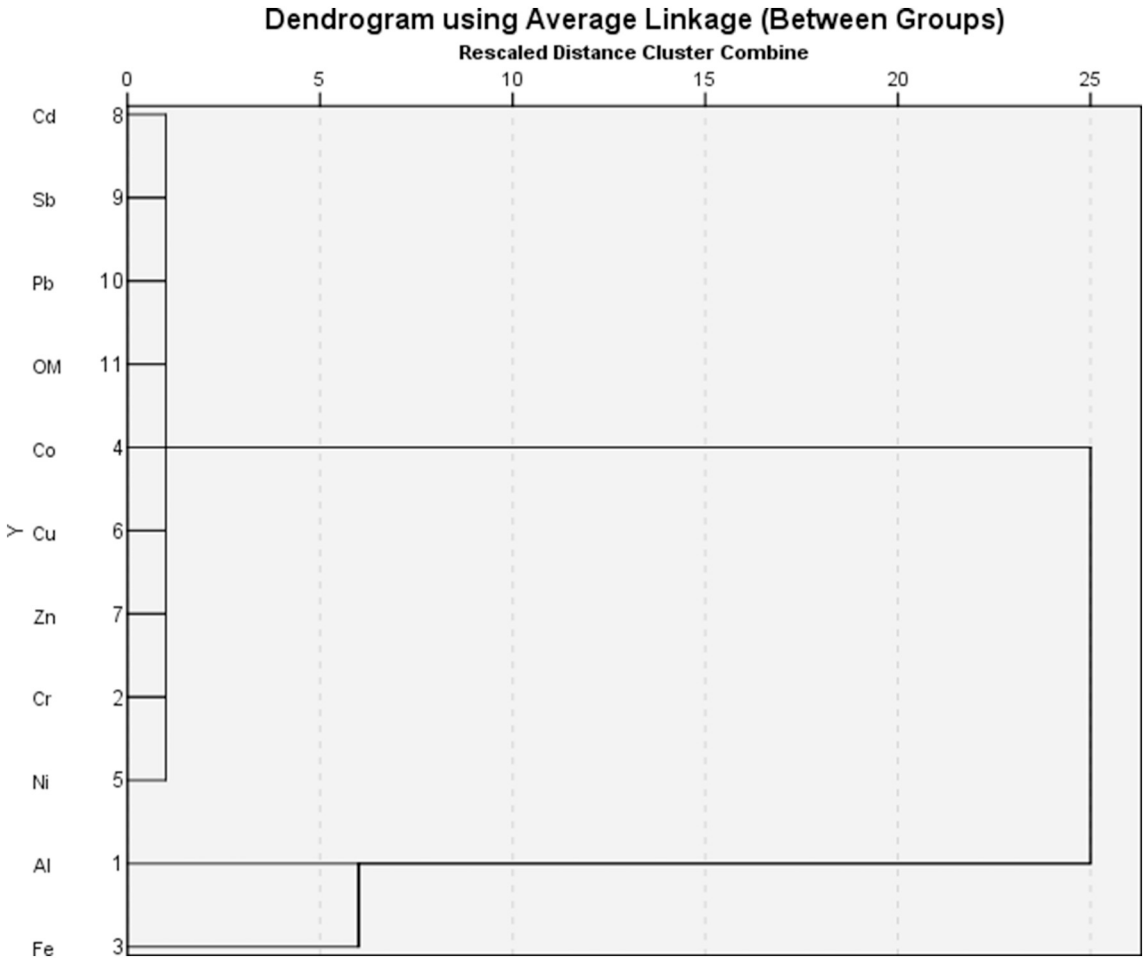

Fig. 3. Dendrogram of the hierarchal clusters analyses of the 10 metals in the 32 surface samples collected along the Jazan coastline.

highest levels of Al, Cr, Fe, Co, Cu, Zn, Cd, Sb, and Pb.

The Pearson's correlation supported the dendrogram results (Table 5) and revealed significantly positive correlations between Pb and each of Cu, Zn, Cd and Pb (r = 0.590, 0.543, 0.811 and 0.903 respectively). Pb may be accumulated mainly in the agricultural soil due to the application of chemical fertilizers (Adimalla et al., 2019). Also, a highly positive correlation is shown between Fe and Al (r = 0.929). In contrast, there is a negative correlation between Fe and Cd (r = −0.115).

The extraction method of principal component analysis (PCA) subdivided the variables into three, accounting for 93.728% of the total variance (Table 6). Each group of elements possibly originates from similar sources. The first component covers 47.901% and presents significant positive loading for Zn, Fe, Ni, Cr, Al, Cu, Sb, and Pb (0.961, 0.806, 0.797, 0.762, 0.724, 0.717, 0.541 and 0.567, respectively). The second component corresponds to 31.118% and presents positive loading for Cd, Sb, and Pb (0.973, 0.811 and 0.729, respectively). The third component covers 14.709% and presents high positive loading for Al (0.669). The source of the highly loading elements in the first component implying that a proportion of Ni, Cr, Cu, Sb, and Pb were from the same source as Fe and Al i.e. lithogenic origin (weathering of crustal materials and atmospheric inputs). The lithogenic source of Cr is related to that, it has been occluded as lattice forms in the residual and the crystalline Fe oxide fraction (Ma and Hooda, 2010). Al and Fe are generally accumulated as oxides or hydroxides in areas of sedimentary rocks. Ni and Cr are derived from soils generated on undifferentiated Quaternary units and their distributions in the earth crust are very similar (Yaylal-Abanuz, 2019). Sb and Pb present positive loading in the first and second groups, implying that they may derive from combined sources, natural (lithogenic) and anthropogenic. The enrichment of Cd, Cr, and Cu in sediments can reflect the level of urbanization, fishing and industrial activities. Cd, Cu, and Zn are often regarded as a marker of agronomic activities in agricultural fields after weathering and erosion, and brought into the coastal areas (Kelepertzis, 2014). The metals in the component plot using a varimax method with the kaiser normalization were distributed into three groups, corresponding to the results from the PCA (Fig. 5). Overall, these data suggest the multi-sources of the HMs on the Jazan coastline sediments, i.e. weathering and erosion, agricultural activities, domestic, industrial, and atmospheric deposition.

4. Conclusions

Analyses of HMs and organic matter in 32 surface sediments from the coastal area, southwest of Saudi Arabia led to the following order of metal concentrations: Al > Fe > Cr > Cu > Zn > Ni > Co > Cd > Sb. Spreading of mangrove trees, as well as algae, and organic fertilizers may have led to the higher content of organic matter. Distribution of HMs within the studied coastal sediments exhibited a fluctuating pattern but there were some individual samples containing high proportion of certain

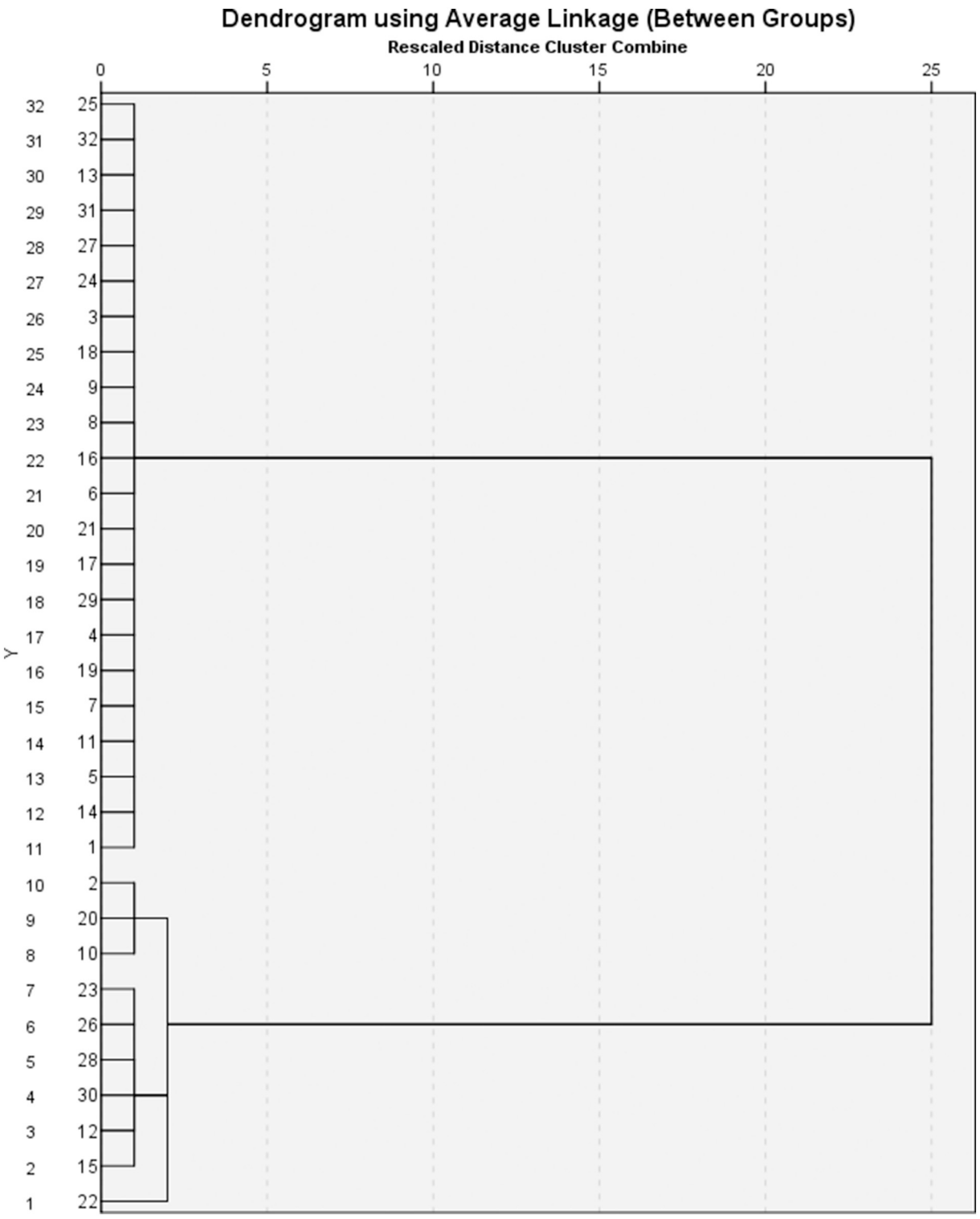

Fig. 4. Dendrogram for hierarchal clusters analyses of 32 surface samples collected along the Jazan coastline.

metals. The average levels of Ni, Zn, Cu, Cr, Sb, Cd, and Pb were less than those of the threshold effect concentration (TEC) of the sediment quality guidelines. Cd recorded very high risk (PERI = 1568), while Cu recorded considerable risk (PERI = 112.18). The enrichment of Cd, Cr, Cu, Zn, Sb, and Ni in mainly reflected anthropogenic source, as well as the lithogenic source in part, while Al and Fe were of lithogenic source. The possible sources of anthropogenic pollutants were urbanization, agricultural and industrial activities, whereas the possible lithogenic sources were sedimentary rocks and soils generated on the mafic rocks of undifferentiated Quaternary units.

Table 5
Correlation matrix of the analyzed metals.

	Al	Cr	Fe	Co	Ni	Cu	Zn	Cd	Sb	Pb
Al	1									
Cr	0.447*	1								
Fe	**0.929****	**0.604****	1							
Co	**0.633****	**0.681****	**0.782****	1						
Ni	0.320	**0.697****	**0.583****	0.405*	1					
Cu	0.214	0.448*	0.209	−0.191	**0.538****	1				
Zn	**0.566****	**0.732****	**0.661****	0.331	**0.791****	**0.820****	1			
Cd	0.106	−0.443*	−0.115	−0.653**	−0.150	0.480**	0.186	1		
Sb	0.372*	0.036	0.200	−0.329	0.172	**0.765****	**0.585****	**0.841****	1	
Pb	**0.589****	−0.031	0.422*	−0.153	0.186	**0.590****	**0.543****	**0.811****	**0.903****	1

Bold a significant positive correlations between metal pairs.
* Correlation is significant at the 0.05 level (2-tailed).
** Correlation is significant at the 0.01 level (2-tailed).

Table 6
Principal component loadings and explained variance for the three components with the varimax normalized rotation.

	Component		
	1	2	3
Zn	**0.961**		−0.168
Fe	**0.806**	−0.284	0.496
Ni	**0.797**	−0.245	−0.354
OM	−0.767	0.248	0.494
Cr	**0.762**	−0.504	−0.216
Al	**0.724**		**0.669**
Cu	**0.717**	0.480	−0.437
Cd	0.118	**0.973**	0.112
Sb	**0.541**	**0.811**	
Co	0.475	−0.766	0.397
Pb	**0.567**	**0.729**	0.342
Percent of variance	47.901	31.118	14.709
Cumulative percent	47.901	79.019	93.728

Extraction method: principal component analysis.
a. 3 components extracted.
Bold a significant positive correlations between metal pairs.

Supplementary data to this article can be found online at https://doi.org/10.1016/j.marpolbul.2020.111125.

CRediT authorship contribution statement

Ali Kahal: Methodology. **Abdelbaset S. El-Sorogy:** Methodology. **Saleh Qaysi:** Methodology. **Sattam Almadani:** Methodology. **Osama M. Kassem:** Methodology. **Ahmed Al-Dossari:** Methodology.

Declaration of competing interest

The authors declare that they have no known competing financial interests or personal relationships that could have appeared to influence the work reported in this paper.

Acknowledgments

The authors extend their appreciation to the Deanship of Scientific Research at King Saud University for funding this work through the Research Group No. (RG-1438-059). Moreover, we thank the anonymous reviewers for their valuable suggestions and constructive comments.

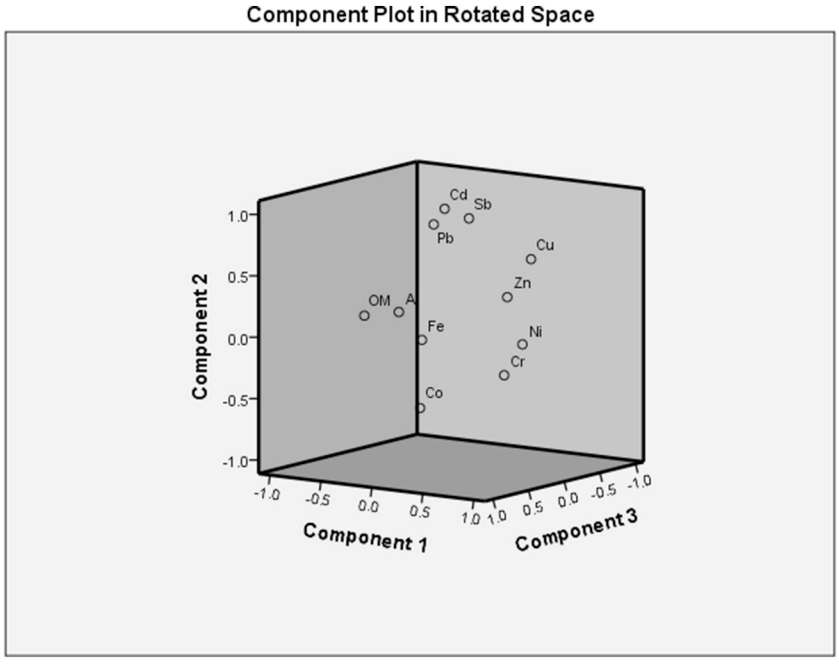

Fig. 5. Three component plots using the varimax method with the kaiser normalization.

References

Abd El-Wahab, M., El-Sorogy, A.S., 2003. Scleractinian corals as pollution indicators, Red Sea coast, Egypt. N. Jb. Geol. Paläont. (Monatsh.) 11, 641–655.

Adimalla, N., Qian, H., Wang, H., 2019. Assessment of heavy metal (HM) contamination in agricultural soil lands in northern Telangana, India: an approach of spatial distribution and multivariate statistical analysis. Environ. Monit. Assess. 191, 246.

Aghadadashi, V., Neyestani, M.R., Mehdinia, A., Bakhtiari, A.R., Molaei, S., Farhangi, M., Esmaili, M., Marnani, H.R., Gerivani, H., 2019. Spatial distribution and vertical profile of heavy metals in marine sediments around Iran's special economic energy zone; arsenic as an enriched contaminant. Mar. Pollut. Bull. 138, 437–450.

Akin, B.S., Kırmızıgu, O., 2017. Heavy metal contamination in surface sediments of Gokcekaya Dam Lake, Eskisehir, Turkey. Environ. Earth Sci. 76, 402.

Alahabadi, A., Malvandi, H., 2018. Contamination and ecological risk assessment of heavy metals and metalloids in surface sediments of the Tajan River, Iran. Mar. Pollut. Bull. 133, 741–749.

Al-Farawati, R., Gazzaz, M., El Sayed, M., El-Maradny, A., 2011. Temporal and spatial distribution of dissolved Cu, Ni and Zn in the coastal waters of Jeddah, eastern Red Sea. Arab J. Geosci. 4, 1229–1238.

Alharbi, T., El-Sorogy, A.S., 2017. Assessment of metal contamination in coastal sediments of Al-Khobar area, Arabian Gulf, Saudi Arabia. J. Afr. Earth Sci. 129, 458–468.

Beltagy, A.I., 1984. Elemental geochemistry of some recent marine sediments from Red Sea. Bull. Inst. Oceanogr. Fish. 10, 1–12.

Birch, G., 2003. In: Woodcoffe, C.D., Furness, R.A. (Eds.), A Scheme for Assessing Human Impacts on Coastal Aquatic Environments Using Sediments. 14 Coastal GIS. Wollongong University Papers in Center for Maritime Policy, Australia.

Dean Jr., W.E., 1974. Determination of carbonate and organic matter in calcareous sediments and sedimentary rocks by loss on ignition: comparison with other methods. J. Sediment. Petrol. 44, 242–248.

Duodu, G.O., Goonetilleke, A., Ayoko, G.A., 2016. Comparison of pollution indices for the assessment of heavy metal in Brisbane River sediment. Environ. Pollut. 219, 1077–1091.

El-Sorogy, A.S., Abdelwahab, M., Nour, H., 2012. Heavy metals contamination of the Quaternary coral reefs, Red Sea coast. Egypt. Environ. Earth Sci. 67, 777–785.

El-Sorogy, A.S., El Kammar, A., Ziko, A., Aly, M., Nour, H., 2013a. Gastropod shells as pollution indicators, Red Sea coast. Egypt. J. Afr. Earth Sci. 87, 93–99.

El-Sorogy, A.S., Nour, H., Essa, E., Tawfik, M., 2013b. Quaternary coral reefs of the Red Sea coast, Egypt: diagenetic sequence, isotopes and trace metals contamination. Arab. J. Geosci. 6, 4981–4991.

El-Sorogy, A.S., Abdel-Wahab, M., Ziko, A., Shehata, W., 2016. Impact of some trace metals on bryozoan occurrences, Red Sea coast, Egypt. Indian J. Geomar. Sci. 45 (1), 86–99.

El-Sorogy, A.S., Al-Kahtany, K., Youssef, M., Al-Kahtany, F., Al-Malky, M., 2018. Distribution and metal contamination in the coastal sediments of Dammam Al-Jubail area, Arabian Gulf, Saudi Arabia. Mar. Pollut. Bull. 128, 8–16.

He, Z.L., Xu, H.P., Zhu, Y.M., Yang, X.E., Chen, G.C., 2005. Adsorption-desorption characteristics of cadmium in variable charge soils. J. Environ. Sci. Health 40, 805–822.

Hökanson, L., 1980. An ecological risk index for aquatic pollution control. A sedimentological approach. Water Res. 14, 975–1001.

Kahal, A., El-Sorogy, A.S., Alfaifi, H., Almadani, S., Ghrefat, H.A., 2018. Spatial distribution and ecological risk assessment of the coastal surface sediments from the Red Sea, northwest Saudi Arabia. Mar. Pollut. Bull. 137, 198–208.

Kelepertzis, E., 2014. Accumulation of heavy metals in agricultural soils of Mediterranean: insights from Argolida basin, Peloponnese, Greece. Geoderma 221 (291), 82–90.

Lin, C., He, M., Liu, S., Li, Y., 2012. Contents, enrichment, toxicity and baselines of trace elements in the estuarine and coastal sediments of the Daliao River system. Chin. J. Geochem. 46, 371–380.

Ma, Y.B., Hooda, P.S., 2010. Chromium, nickel and cobalt. In: Hooda, P.S. (Ed.), Trace Elements in Soils. Wiley, Chichester (c).

Mao, L., Liu, L., Yan, N., Li, F., Tao, H., Ye, H., Wen, H., 2019. Factors controlling the accumulation and ecological risk of trace metal(loid)s in river sediments in agricultural field. Chemosphere. https://doi.org/10.1016/j.chemosphere.2019.125359.

Mil-Homens, M., Vale, C., Raimundo, J., Pereira, P., Brito, P., Caetano, M., 2014. Major factors influencing the elemental composition of surface estuarine sediments: the case of 15 estuaries in Portugal. Mar. Pollut. Bull. 84, 135–146.

Müller, G., 1981. Die schwermetallbelastung der sediment des Neckars und Seiner Neben flusse: eine Bestandsaufnahme. Chem. Zeit. 105, 157–164.

Nour, H., El-Sorogy, A.S., 2017. Distribution and enrichment of heavy metals in Sabratha coastal sediments, Mediterranean Sea, Libya. J. Afr. Earth Sci. 134, 222–229.

Nour, H., El-Sorogy, A.S., Abdel-Wahab, M., Almadani, S., Alfaifi, H., Youssef, M., 2018. Assessment of sediment quality using different pollution indicators and statistical analyses, Hurghada area, Red Sea coast, Egypt. Mar. Pollut. Bull. 133, 808–813.

Nour, H.N., El-Sorogy, A.S., Abd El-Wahab, M., Nouh, E., Mohamaden, M., Al-Kahtany, Kh., 2019. Contamination and ecological risk assessment of heavy metals pollution from the Shalateen coastal sediments, Red Sea, Egypt. Mar. Pollut. Bull. 144, 167–172.

Pejman, A., Bidhendi, G.N., Ardestani, M., Saeedi, M., Baghvand, A., 2015. A new index for assessing heavy metals contamination in sediments: a case study. Ecol. Indic. 58, 365–373.

Qing, X., Yutong, Z., Shenggao, L., 2015. Assessment of heavy metal pollution and human health risk in urban soils of steel industrial city (Anshan), Liaoning, Northeast China. Ecotoxicol. Environ. Saf. 120, 377–385. https://doi.org/10.1016/j.ecoenv.2015.06.019.

Ruiz-Compean, P., Ellis, J., Cúrdia, J., Payumo, R., Langner, U., Jones, B., Carvalho, S., 2017. Baseline evaluation of sediment contamination in the shallow coastal areas of Saudi Arabian Red Sea. Mar. Pollut. Bull. 123, 205–218.

Salem, D.M., Khaled, A., El Nemr, A., El-Sikaily, A., 2014. Comprehensive risk assessment of heavy metals in surface sediments along the Egyptian Red Sea coast. Egypt. J. Aquat. Res. 40, 349–362.

Tang, Z., Chai, M., Cheng, J., Jin, J., Yang, Y., Nie, Z., et al., 2017. Contamination and health risks of heavy metals in street dust from a coal-mining city in eastern China. Ecotoxicol. Environ. Saf. 138, 83–91.

Taylor, S.R., 1964. Abundance of chemical elements in the continental crust: a new table. Geochim. Cosmochim. Acta 28, 1273–1285.

Turekian, K.K., Wedepohl, K.H., 1961. Distribution of the elements in some major units of the earth's crust. Geol. Soc. Am. 72, 175–192.

US EPA, 1983. Methods for Chemical Analysis of Water and Wastes. Environmental Monitoring and Support Laboratory. United States Environmental Protection Agency, Office of research and development, Washington, DC20460, pp. 375p.

Usman, A.R.A., Alkredaa, R.S., Al-Wabel, M.I., 2013. Heavy metal contamination in sediments and mangroves from the coast of Red Sea: Avicennia marina as potential metal bioaccumulator. Ecotoxicol. Environ. Saf. 97, 263–270.

Yaylal-Abanuz, G., 2019. Application of multivariate statistics in the source identification of heavy-metal pollution in roadside soils of Bursa, Turkey. Arab. J. Geosci. 12, 382.

Youssef, M., El-Sorogy, A.S., 2016. Environmental assessment of heavy metal contamination in bottom sediments of Al-Kharrar lagoon, Rabigh, Red Sea, Saudi Arabia. Arab. J. Geosci. 9, 474.

Yu, T., Zhang, Y., Meng, W., Hu, X.N., 2012. Characterization of heavy metals in water and sediments in Taihu Lake, China. Environ. Monit. Assess. 184, 4367–4382.